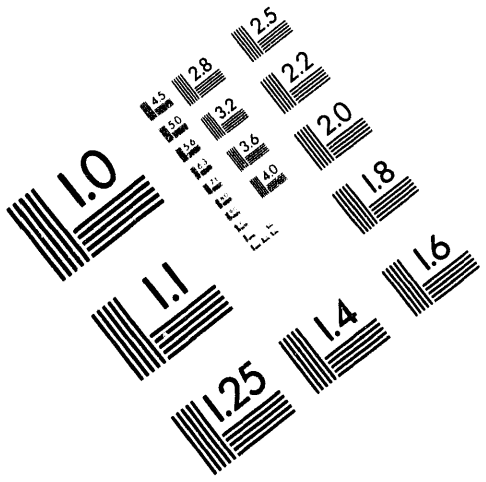

Association for Information and Image Management
1100 Wayne Avenue, Suite 1100
Silver Spring, Maryland 20910
301/587-8202

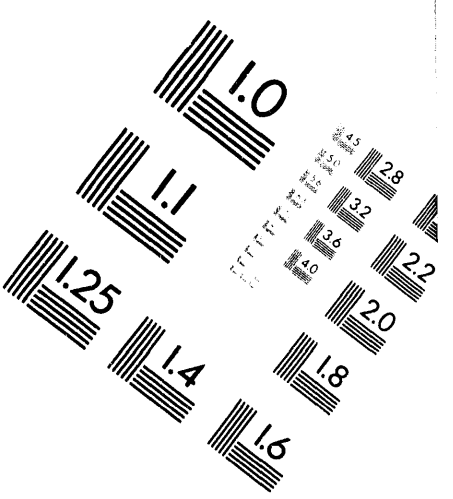

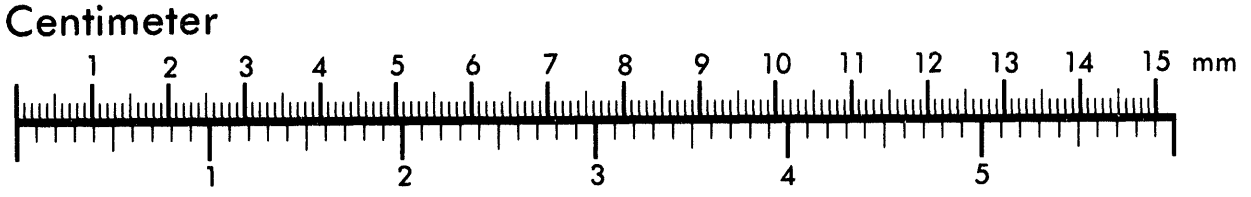

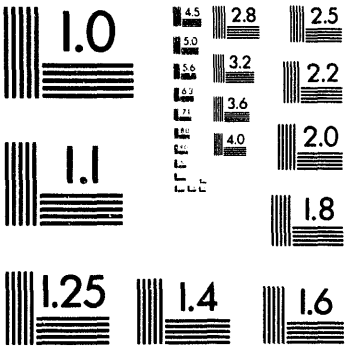

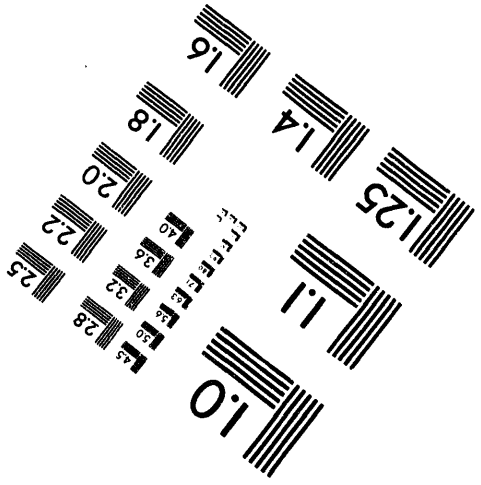

MANUFACTURED TO AIIM STANDARDS
BY APPLIED IMAGE, INC.

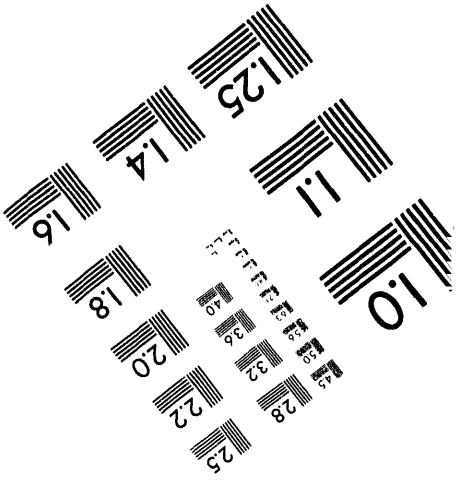

1 of 1

Conf-940553--67

SATURATION LEVELS AND TRENDS IN THE UNSATURATED ZONE, YUCCA MOUNTAIN, NEVADA

Philip H. Nelson
U.S. Geological Survey
Box 25046, Federal Center, MS 964
Denver, Colorado 80225
303 236 1322

ABSTRACT

Water content and porosity within the unsaturated zone at Yucca Mountain are computed from the caliper, density, and epithermal neutron logs obtained in 15 WT-boreholes. Separation between the water content and porosity logs clearly demarcate the lithophysal zones within the Topopah Spring Member of the Paintbrush Tuff. Lithophysal and nonlithophysal zones constitute regionally correlatable intervals across the area penetrated by the WT-boreholes. Lithophysal abundance appears to be nearly zero in the lower lithophysal zone in the southernmost boreholes. Total porosity increases as lithophysal abundance increases, and water saturation decreases in the zones with high lithophysal abundance. Averages of water content for two lithophysal zones in the Topopah Spring Member of the Paintbrush Tuff show that water content decreases with height above the static water level; the trends in water content versus elevation are a function of geological zone. Thus, the pore size distribution spectrum appears to be preserved in the lithophysal zones.

INTRODUCTION

The unsaturated zone at Yucca Mountain, Nevada, consists of interstratified nonwelded tuffs, which are locally altered to zeolites and clays, and welded tuffs which have laterally extensive lithophysal and nonlithophysal zones (Fox et al., 1990). The vertical heterogeneity and lateral homogeneity in rock types control the physical and hydrological properties. Water content and porosity within the unsaturated zone at Yucca Mountain can be quantified using geophysical logs. A log-based approach offers the advantage of in-situ measurements, continuous throughout a borehole. Water content and porosity can be determined with a pair of geophysical logs, such as the density and dielectric logs (Nelson, 1993), or with the density and epithermal neutron logs, as outlined in this paper.

The density tool incorporates a source of gamma radiation and two detectors on a sidewall pad; scattering of gamma rays causes the count rate at each detector to decrease as rock density increases. Laboratory calibration of the tool requires that count rate be related to density, with consideration for the effects of hole size, gap, and fluid type. The epithermal neutron tool, designated "ENP", incorporates a source of neutrons and a single epithermal neutron detector on a sidewall pad pressed against the wall of the borehole. Moderation of energetic neutrons by light elements in the rock (principally hydrogen) causes the count rate of epithermal neutrons at the detector to decrease as hydrogen content increases. Laboratory calibration of the ENP, discussed in more detail below, relates the count rate to hydrogen (water) content, with consideration for the effects of hole size, gap, rock type, and rock density.

In this paper, logs from 15 WT-boreholes, drilled to monitor the depth of the static water level, are presented. (For brevity, the USW prefix in the full borehole name is dropped.) These boreholes (1) provide good geographical coverage of Yucca Mountain (Figure 1), (2) were drilled with a bit size of 8.75 inches (with the exception of WT-6, 6.75 inches), (3) were drilled within a one year time period during 1983 and 1984, and (4) were logged with a fairly consistent set of logging tools. All the WT-boreholes were logged with the same Birdwell density tool, LAJD-8001, #6. Three epithermal neutron tools were used: Birdwell LABE-6001, #20, #21, and #23.

Erroneous high count (low-density) spikes on the density log (Figure 2) must be treated before the log can be used. The spikes occur in a rough, air-filled borehole wherever a gap, or separation between the tool face and the borehole wall exists (Nelson et al., 1991). In this analysis, the effect of gap is overcome by spline fitting a curve to the high density edge of the density log, thereby interpolating across the erroneous low density spikes. High-count spikes also occur on the epithermal neutron log where gaps exist, consequently the neutron log is also treated with a spline fit.

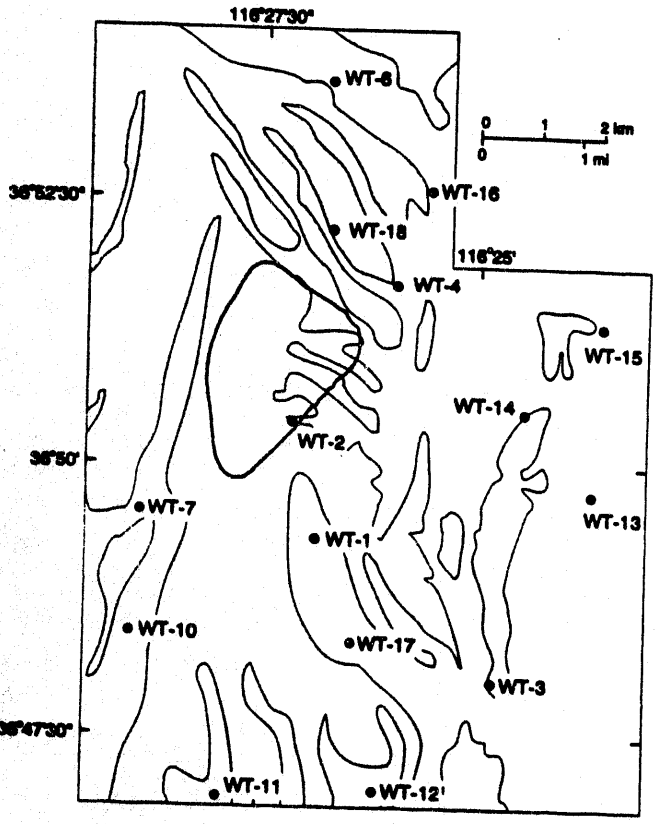

Figure 1. Location of WT series of boreholes at Yucca Mountain, Nevada. White areas are alluvium. Potential repository location outlined in black.

WATER-FILLED AND TOTAL POROSITY

To calibrate the ENP, Hearst (1979) and Hearst et al. (1981) developed a Hydrogen Content Test Facility (HCTF) at the Nevada Test Site constructed of aluminum boxes containing alumina, silica, and water. Twelve cells provide 12 mixtures of density and water content spanning the ranges of 0.85 to 2.64 g/cm^3 and 0 to 100% water volume. The HCTF provides a flat wall to simulate the very large boreholes and an empty 30-cm square column simulating a 30-cm borehole. Using the HCTF calibrations to compute water content has some advantages for our work. Calibrations were made in the HCTF during October 1983 through May 1984, and so are valid for the logs considered here. The calibrations were done on materials chemically similar to the tuffs, so that no additional transform to account for rock type dissimilarites is required. Calibration cells were partially saturated, so air was present in the media and does not require separate accounting. Calibration cells and resulting algorithms incorporate the effect of varying density, which does affect the relationship between counting rate and water content, particularly at water contents below 0.2.

An algorithm relating count rate and hydrogen content for zero gap is

$$y = \ln(N) = \alpha_1(1 + \alpha_2\rho_b)\exp(\alpha_3 I_H) + \alpha_4 \quad (1)$$

where N is the measured count rate (expressed in API units), y is the natural logarithm of N, I_H is hydrogen index, ρ_b is the bulk density, and α_i are coefficients determined by fitting the function to the calibration data (Hearst et al., 1981).

Hydrogen index I_H is determined from the ENP log by interpolation using eq. 1, which also requires a density measurement from the density log and α_i coefficients for a 12-inch air-filled borehole. Adjustment is then made for hole size using the caliper measurement.

As indicated by equation 1, the ENP responds to hydrogen content rather than the desired water content. If hydrogen exists only in water in pore space, then the hydrogen index I_H is equivalent to water-filled porosity ϕ_w, which is the ratio of water-filled pore space to total rock volume and is often referred as volumetric moisture content. The relationship between bulk density measured by the density log and ϕ_w is

$$\rho_b = \rho_g(1 - \phi_t) + \rho_w\phi_w + \rho_a\phi_a \quad (2)$$

where ρ_g is the grain density, ρ_w is the water density, ρ_a is the air density, ϕ_t is total porosity, and ϕ_a is the air-filled porosity. The last term can be ignored because the air density is nearly zero, and the solution for total porosity is

$$\phi_t = (\rho_g - \rho_b + \rho_w\phi_w)/\rho_g \quad (3)$$

Thus, once ϕ_w is determined from equation 1 by equating it to I_H, total porosity can be determined from equation 3. Water saturation is computed as the ratio ϕ_w/ϕ_t.

This derivation assumes that hydrogen index I_H is equivalent to water-filled porosity ϕ_w. Because zeolites and clays contain hydrogen, I_H will be greater than true ϕ_w in altered zones, and can even be greater than ϕ_t. Thus, a comparison of I_H (hereafter referred to as ϕ_w) and ϕ_t can serve to delineate zeolites and clays.

RESULTS FROM BOREHOLE WT-2

Caliper, density, and ENP logs and the computed ϕ_w, ϕ_t, and water saturation extend in borehole WT-2 from borehole depths of 55 feet to 2000 feet, a depth some 60 feet short of total depth (Figure 2). The ENP log dominates the ϕ_w response, and the ρ_b log dominates the ϕ_t response, although equations 1 and 3 show that both the ρ_b

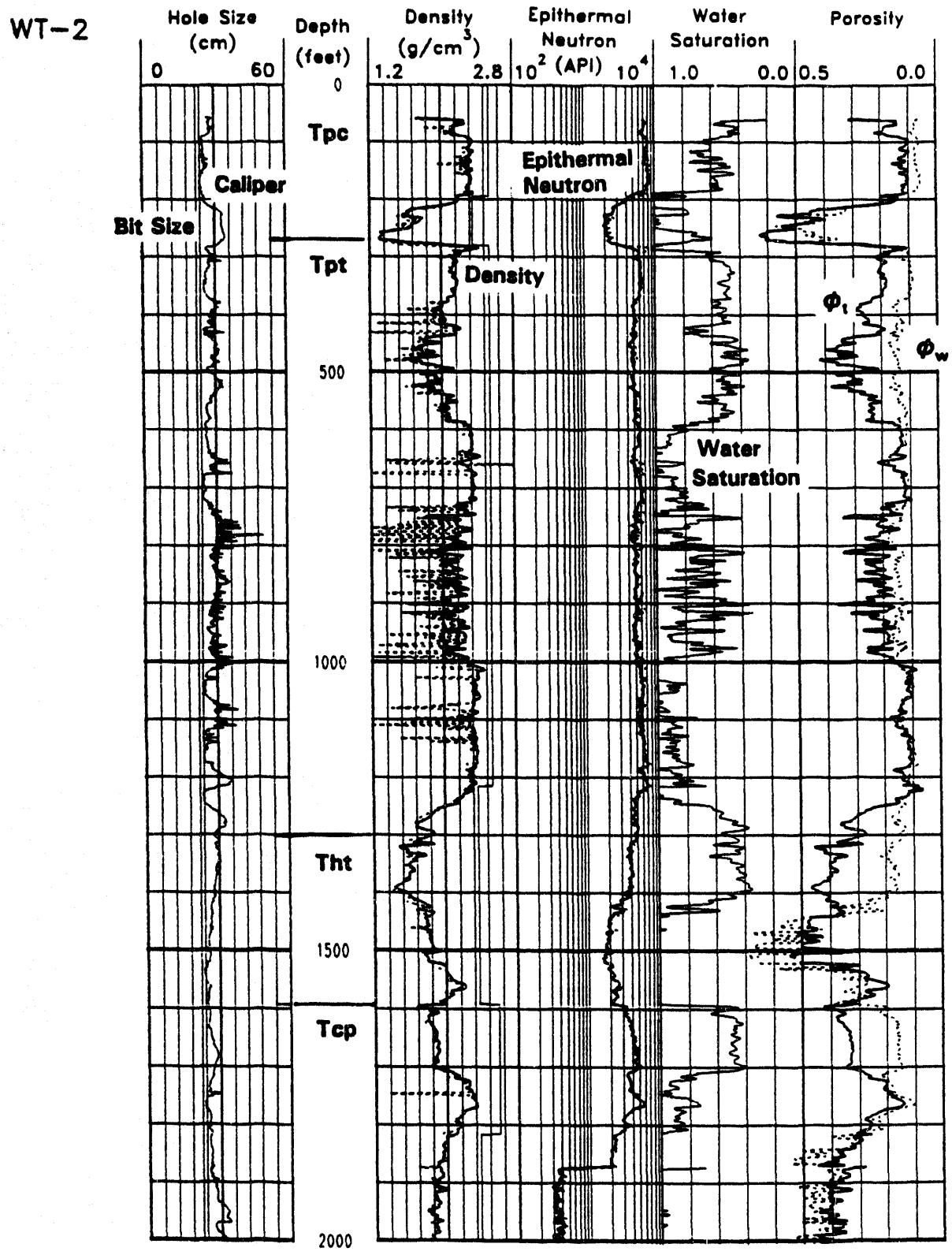

Figure 2. Caliper, density, and epithermal neutron logs and calculated water saturation, total porosity (ϕ_t), and water-filled porosity (ϕ_w) in borehole WT-2. Grain density used for calculations is shown immediately to the right of density. For consistency with the density and neutron logs, ϕ_w and ϕ_t increase in value to the left and are expressed as volume fractions. Static water level is at 1873 feet.

and ENP logs are used to compute ϕ_w and ϕ_t. Air-filled porosity is represented by the separation between ϕ_w and ϕ_t. Downhole variations in logged and computed values, discussed next in order of increasing depth, are controlled by lithology.

In the welded portion of the Tpc, 55 to 195 feet, total porosity is 0.12 and saturation is 0.60. (Geologic zones will be referred to by symbols listed in Fig. 3.) The non-welded/bedded tuff spanning the contact between Tpc and Tpt (195 to 282 feet in Figure 2) occurs in all the WT holes and is quite porous ($\sim$0.40 to 0.50). The high apparent water saturations in this unit are considerably higher than laboratory data in nearby borehole UZ-16 (A. Flint, pers. comm.). This discrepancy could be due to the presence of clay and zeolite minerals or due to improper compensation of the ENP data for hole washout and/or low density.

The lithophysal zones of the Tpt (365 - 585 and 745 - 1000 feet) are easily recognized from caliper spikes, low density spikes, and air-filled porosity, e.g., the separation between ϕ_w and ϕ_t. A high amount of air-filled porosity can be used to help define and correlate the lithophysal sections of the Tpt from borehole to borehole. In welded and devitrified tuff, saturation is controlled primarily by variation in ϕ_t, which increases as lithophysal abundance increases. Saturation is 80 to 100% in the middle non-lithophysal zone and drops to about 50% in the zones with high lithophysal abundance. The lower saturation is attributed to drainage of the large pores and lithophysae.

Continuing with the lower half of WT-2 (Figure 2), zeolitization is evident where ϕ_w exceeds ϕ_t from 1440 to 1522 feet and from 1815 to deeper than 2000 feet. Two high porosity - low saturation zones can be observed in the upper intervals of Tht and Tcp. On the basis of cuttings description, the interval from 1222 to 1416 is described as nonwelded and vitric; the interval from 1593 to 1710 as non-to-poorly welded and with vapor-phase alteration (D. Buesch, pers. comm.). In the welded center of Tcp, 1720 to 1770 feet, total porosity declines to less than 0.20 and saturation is close to 100%.

CORRELATION OF LITHOPHYSAL ZONES

The computed porosity and water content in 15 WT-boreholes are plotted from west to east in three groups: north (Fig. 3), central (Fig. 4), and south (Fig. 5). Wherever possible, the logs are tied to the top of Tpt. The lithophysal zones and the highly altered (zeolitic) zones have been picked from the relationship between ϕ_t and ϕ_w and indicated at the left of each column.

The upper lithophysal zone can be readily correlated from hole to hole in 12 of the 15 boreholes. The three exceptions are WT-6 (Fig. 3), where the upper Tpt was not penetrated, WT-10 (Fig.5), where the upper lithophysal zone lies below the static water level (SWL), and WT-7 (Fig.4). Borehole WT-7, in the southwest corner of the area, shows none of the characteristic split between ϕ_t and ϕ_w. Thus, in WT-7 and probably in WT-10 as well, lithophysae appear to be either poorly developed or else nearly filled with secondary minerals.

The lower lithophysal zone occurs in 13 of the 15 holes. The two exceptions are due to no penetration (WT-6, Fig. 4, and WT-10, Fig. 5. Lack of air-filled porosity in four boreholes (WT-7, Fig. 4; WT-11, -17, -12, Fig. 5) indicates that lithophysae are either not present or else filled with secondary minerals in an area south and west of WT-1. The short intercept in WT-3 indicates that the lower lithophysal zone is present in that hole.

CONTROLS ON WATER CONTENT

The dominant controls on water content in the unsaturated zone are expected to be gravitational potential and capillary tension. Capillary tension depends upon the pore size distribution, which can be a function of the rock unit. To examine these effects, the Tpt was divided into five rock units, with boundaries picked from the logs of Figures 3-5. Although the detailed geological description is more complicated, basically the five zones are the upper and lower lithophysal zones (designated ul and pll in Fig. 6a), bounded by the upper, middle, and lower non-lithophysal zones (rn, pmn, pln in Fig. 6b). Average water content (ϕ_w) is calculated for the five zones in each WT borehole.

With the water content averages identified by zone, the control exerted by lithological zone and by height can be identified. The two lithophysal zones (ul and pll) show a systematic decrease in water content as the height of a given zone increases above SWL and also show a clear offset between the upper and lower lithophysal zones (Fig. 6a). However, the scatter is much greater among the nonlithophysal zones, the decrease with height (if any) is much less clearcut, and grouping by zone is poorly defined (Fig. 6b). Thus lithology and height above SWL control the water content in the lithophysal zones of the Tpt, but much less can be said regarding the nonlithophysal zones.

CONCLUSIONS

The spatial variation of ϕ_w and ϕ_t demonstrate strong lithologic control. Dominant uncertainties in the estimate of ϕ_w include an incomplete calibration of the ENP and the

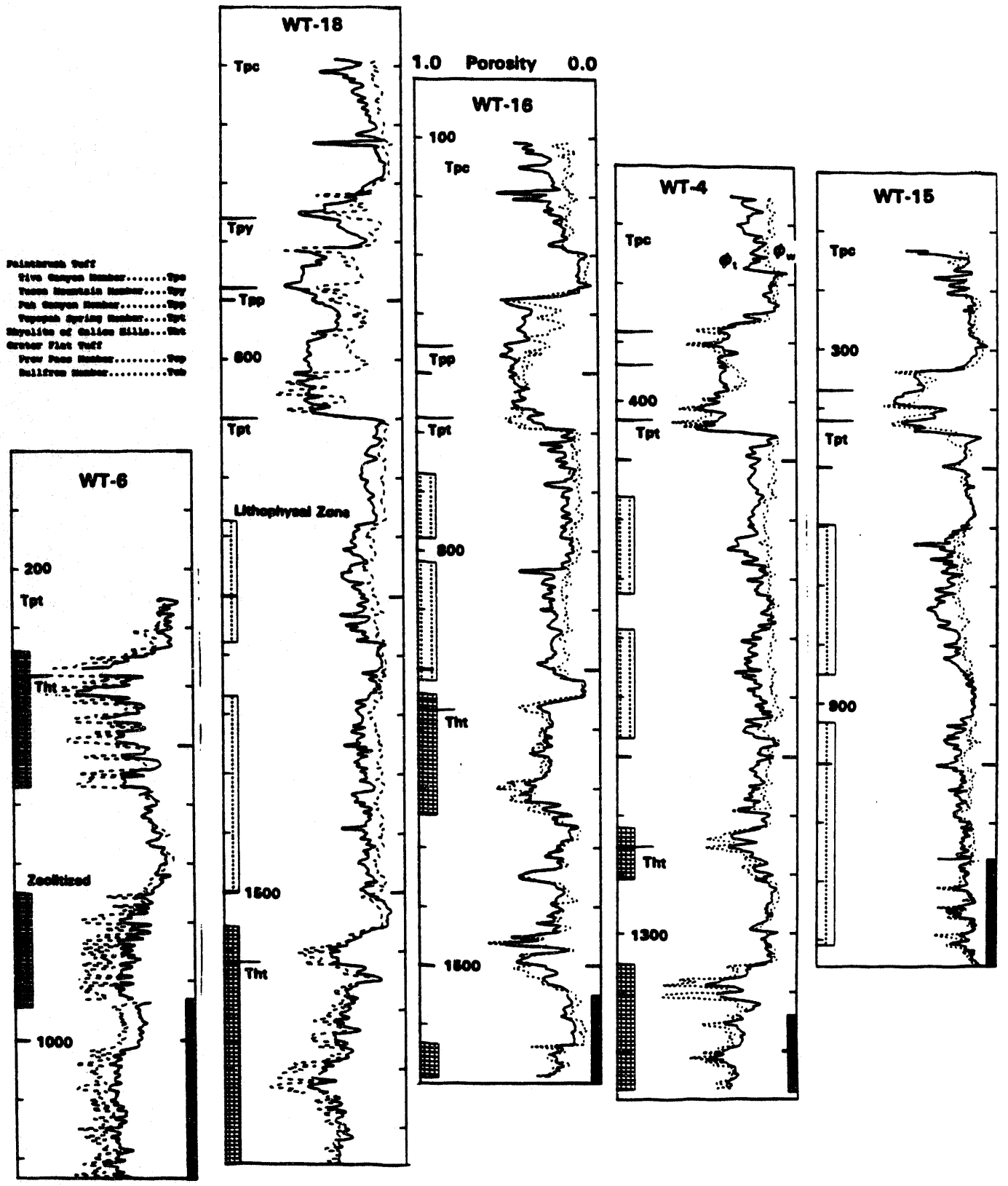

Figure 3. Total porosity (ϕ_t, solid line), and water-filled porosity (ϕ_w, dashed line) in five northern WT-holes, aligned at top of Tpt. Lithophysal zones, picked from logs, are indicated by dotted boxes. Highly zeolitized zones are indicated by boxes with waffle grid. Black bar indicates static water level. Depth is in feet below surface.

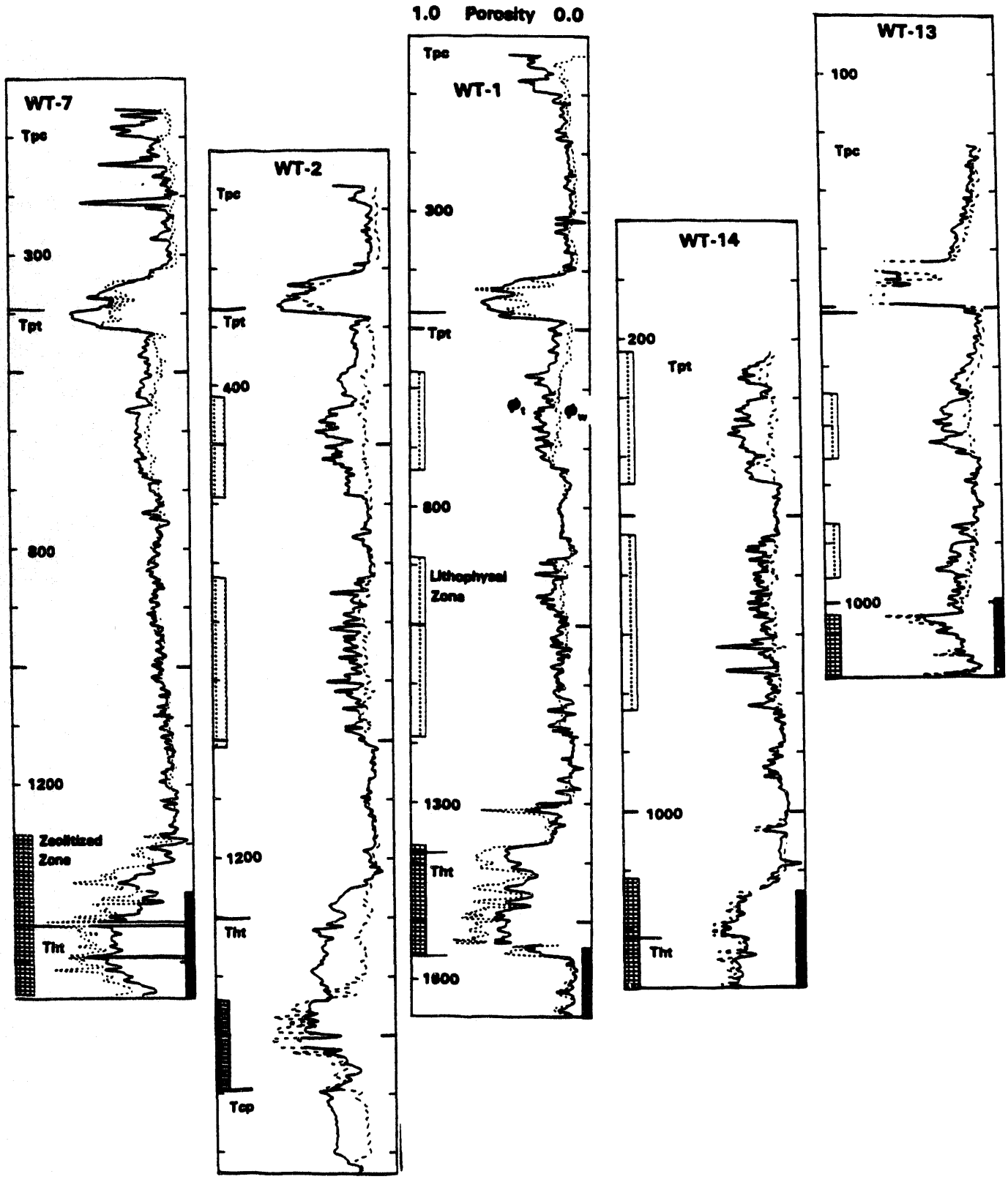

Figure 4. Total porosity (ϕ_t, solid line), and water-filled porosity (ϕ_w, dashed line) in five central WT-holes, aligned at top of Tpt. Black bar indicates static water level. Depth is in feet below surface.

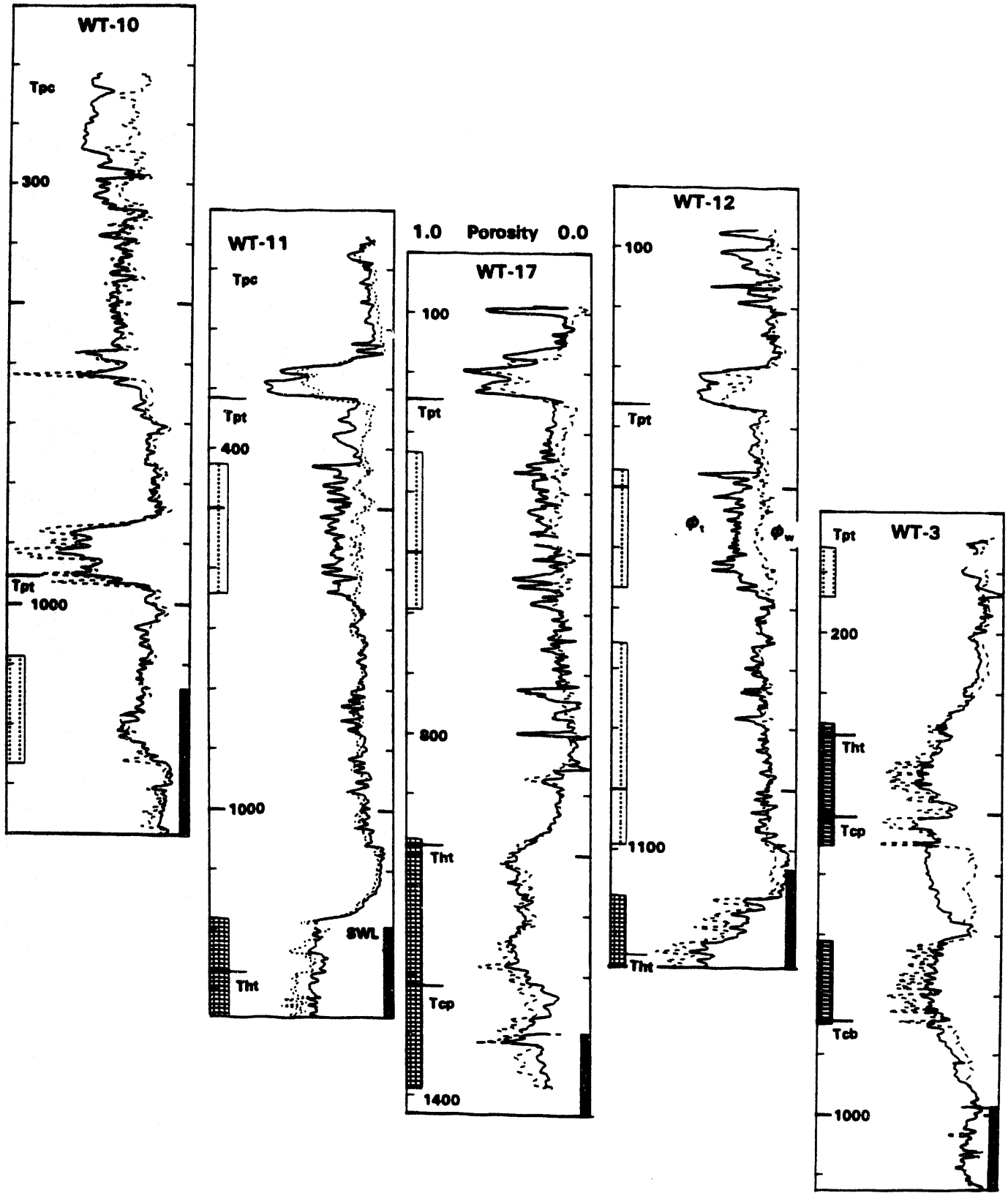

Figure 5. Total porosity (ϕ_t, solid line), and water-filled porosity (ϕ_w, dashed line) in five southern WT-holes, aligned at top of Tpt (WT-10 is shifted down and WT-3 is shifted up relative to others). Black bar indicates static water level. Depth is in feet below surface.

likely presence of small amounts of hydrogenous clay, even in the welded units. Despite these uncertainties, the computed logs of Figures 3-5 are certainly valid for examining vertical variations of water content and saturation, and because a uniform logging program was used in the WT-holes, are considered valid for examining lateral variations as well. Estimates of ϕ_w and ϕ_t from dielectric and density logs (Nelson, 1993), not shown here, generally confirm the trends of Figures 3-5.

Total porosity increases as lithophysal abundance increases, and saturation drops in the zones with high lithophysal abundance. Due to water within the zeolite structure, zones of zeolitic alteration are characterized by apparent water content in excess of total porosity. Average water content in the lithophysal zones in Tpt decreases with height above the SWL. Thus, the pore size distribution is preserved within the lithophysal subzones over the area penetrated by the WT-boreholes.

Acknowledgements. J.E. Kibler assisted with data reduction and plotting. Careful reviews by D. Buesch and P. Tucci led to improvements in the manuscript.

REFERENCES

Fox, K.F., Jr., Spengler, R.W., and Myers, W.B., 1990, Geologic framework and Cenozoic evolution of the Yucca Mountain area, Nevada, *in* Proc. of Intl. Symposium on Unique Underground Structures, vol. 2, R.S. Sinha, ed., 18 p.

Hearst, J. R, 1979, Calibration of a neutron log in partially saturated media: Transactions of 20th Annual Logging Symposium, Society of Prof. Well Log Analysts, paper B, 28 p.

Hearst, J. R, Kasameyer, P.W. and Dreilling, L.A., 1981, Calibration of a neutron log in partially saturated media, Part II: error analysis: Transactions of 22nd Annual Logging Symposium, Society of Prof. Well Log Analysts, paper QQ, 47 p.

Nelson, P.H., Muller, D.C., Schimschal, U., Kibler, J.E., 1991, Geophysical logs and core measurements from forty boreholes at Yucca Mountain, Nevada: U.S. Geological Survey, Geophysical Investigations Map GP-1001, 64 p., 40 plates.

Nelson, P.H., 1993, Estimation of water-filled and air-filled porosity in the unsaturated zone, Yucca Mountain, Nevada, *in* Proc. of the 4th Annual International Conference on High-Level Radioactive Waste Management, Am. Nuclear Society, vol 1, p. 949-954.

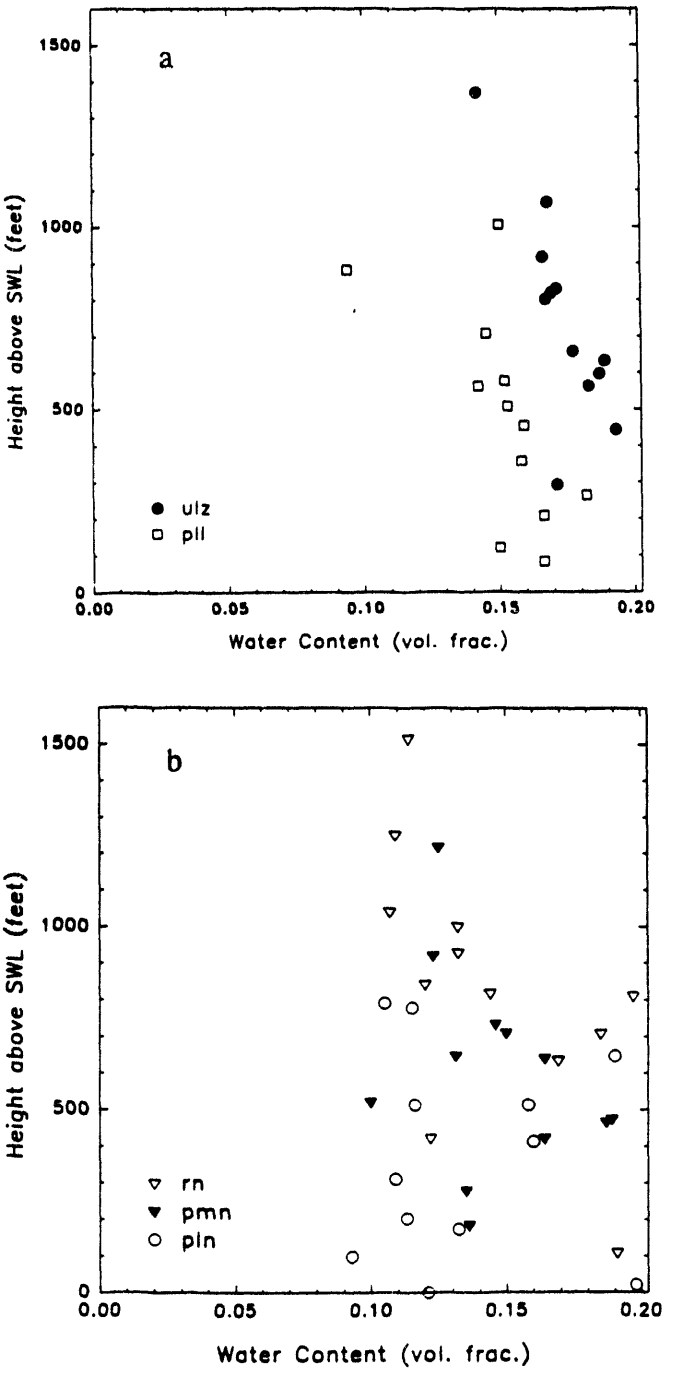

Figure 6. Average water content for (a) lithophysal and (b) nonlithophysal zones in Topopah Spring Member, versus height above static water level. Each symbol represents the vertical average over a lithologic zone within a WT-borehole. Nomenclature: rn, crystal-rich, non-lithophysal zone; ul, upper lithophysal zone; pmn, crystal-poor, middle non-lithophysal zone; pll, crystal-poor, lower lithophysal zone; pln, crystal-poor, lower nonlithophysal zone.

DATE
FILMED
8/4/94

END